

Evaluating The Biostimulation Effect Of Diode Laser 650 Nm Combined With TEMPO Oxidized Nano-Cellulose Mixed With Biphasic Tricalcium Phosphate On Bone Healing: Experimental Animal Study

Ahmed Fouad Serageldin Allam¹, Ahmed Abbas Zaky², Hanaa Mohammad Elshenawy³, Engie M. Safwat⁴, Mohammad L. Hassan⁵, Mohamed Abdullah Mohamed Nassar⁶, Said K. Taha⁷

1. Research Assistant, Surgery and Oral Medicine Department. Oral & Dental Research Institute, National Research Centre (NRC).
2. Professor and Head of Medical Application of Laser Department. National Institute of Laser Enhanced Science - Cairo University.
3. Professor, Oral & Dental Laser Applications. Surgery & Oral Medicine Department. Oral & Dental Research Institute, National Research Centre (NRC).
4. Associate Professor, Restorative and Dental Materials Department, National Research Centre.
5. Professor at Cellulose and Paper Department. Centre of Excellence for Advanced Sciences, Advanced Materials and Nanotechnology Groups, National Research Centre (NRC).
6. Researcher, Restorative and Dental Materials Department, Oral and Dental Research Institute, National Research Centre (NRC).
7. Researcher, Surgery and Oral Medicine Department, Oral and Dental Research Institute, National Research Centre (NRC).

Email: Allamahmed@hotmail.com

DOI: 10.47750/pnr.2023.14.S02.289

Abstract

Objective The purpose of the current study was to evaluate the effect of Diode laser 650 nm, mineralized Nano-cellulose graft material, and their combination on bone healing using Masson's Trichrome stain. **Methods** a total of 18 adult male white New Zealand rabbits were used. Two circular full cortical bone defects were drilled in each tibia, creating four bony defects in each rabbit, representing the four main groups of the study; group A (negative control), group B (filled with Tetramethyl pyridine oxyl "TEMPO" oxidized Nano-cellulose combined with Nano Amorphous-calcium-phosphate "nACP", group C (combination group filled with experimental material and subjected to laser), group D (subjected to Diode laser 650 nm). In groups C and D, bony defects were subjected to laser irradiation during surgery, then repeated every other day for two weeks. Animals were sacrificed after two weeks and one month, histological samples were examined by Masson's Trichrome stain. **Results** after two weeks, group D recorded the greatest mean area percent of osteoid, while group C recorded the lowest value. After one month, groups A and D showed full closure of the defects, groups B and C showed partial defect closure with retained bone graft material, with group B recording the greatest mean area percent of osteoid formation, whereas group C recorded the lowest value. **Conclusion** Diode laser biostimulation improved bone defects' healing. Mineralized Nano-cellulose as a bone substitute showed a delayed effect in bone healing, and graft material resorption. The combination of LLLT with the mineralized Nano-cellulose material had no positive outcome on bone defect healing.

Keywords: Rabbit, Amorphous-calcium-phosphate, LLLT, Masson's Trichrome, bone healing, Nano-cellulose

Introduction

Bone is capable of repair through physiologic remodeling or healing processes. Bone regeneration techniques can be incorporated into this process to assist or stimulate bone growth. (Arvidson et al, 2011; Qu et al, 2012) Various techniques, including the use of barrier membranes and graft material, have been proposed for the management of bone defects. There has been Continuous attempts to create new bone graft materials with improved bioactivity for tissue engineering purposes, using composites of cellulose Nano-materials and calcium phosphate particles. (Acar et al, 2016)

Calcium phosphate compounds, as artificial bone graft substitutes, are in high use because of their biocompatibility, porosity, different rates of dissolution, handling characteristics, chemical & physical resemblance to bone mineral, relatively low cost and availability in large quantities. (Hou et al, 2022)

Biphasic calcium phosphate (BCP) as one of the bioactive ceramic materials, is considered the gold standard of bone substitutes composed of a mixture of two different calcium phosphate phases at different ratios: hydroxyapatite (HA) and Tricalcium phosphate (TCP). (*Leotot et al, 2015*)

Cellulose is a form of natural polysaccharide composed of many hydroxyl groups that connect with one another or with the hydroxyl groups of nearby polymer chains via hydrogen bonding. Growing interest has been shown in Nano-cellulose as a novel nanomaterial with unique hydrogel-like characteristics. (*Yao and Xu, 2014*).

Nano-cellulose hydrogel prepared from rice straw exhibited a biocompatible response regarding non-toxic effect on osteoblast-like cells, and its capacity to induce ossification as evidenced by the positive alkaline phosphate assay. Tetramethyl pyridine oxyl (TEMPO) oxidized Nano-fibrillated cellulose extracted from rice straw, mixed with biphasic Tricalcium phosphate, proved to be a successful bone graft material. (*Safwat et al, 2018*)

LLLT (Low Level Laser Therapy) is the application of red and near infra-red light over wounds or lesions to improve wound and soft tissue healing, reduce inflammation and provide relief for both acute and chronic pain. Increased speed, quality, and tensile strength of tissue repair are achieved by the application of LLLT, consequently promoting the healing process. Low-power laser irradiation considerably increases the number of viable osteocytes in the irradiated bone in hard tissues, by having a positive impact on the bone matrix and producing highly reactive & vital bone tissue. (*De Souza et al, 2012; Neto et al, 2021*)

Rabbit is one of the most commonly used animal models, and it ranks first among all the animals used for musculoskeletal research. According to studies, rabbits and humans have similar mid-diaphyseal bone fracture toughness and bone mineral density. Rabbits are easily available, easy to house and handle, and they have faster skeletal change and bone turnover. (*Ye Li et al, 2015*)

This study aims to evaluate the effect of LLLT, mineralized Nano-cellulose graft material and their combination on bone healing using Masson's trichrome stain.

Materials and methods

Experimental Animals This study was applied on 18 adult healthy white male New Zealand rabbits, weighing 3-4 kgs. The study protocol was approved by the medical research ethics committee of the National Research Centre (NRC #19076). Housing and surgery took place at the animal house unit (Faculty of medicine, Cairo University, Egypt). Rabbits were raised in individual metal cages, and offered food & water.

Bone graft material preparation The experimental material used was a mixture of Tetramethyl pyridine oxyl (TEMPO) oxidized Nano-cellulose hydrogel prepared according to *Safwat et al, 2018* (patent under registration no 2015/1980, Ministry of scientific research, Academy of scientific research & technology, Egypt), and Nano Amorphous calcium phosphate (nACP) (Sigma Aldrich Chemical Company St. Louis, USA). Nano-cellulose hydrogel (2% dry weight) and Nano Amorphous Calcium Phosphate were mixed in 1:1 weight ratio, and homogenized using CAT uni-drive 1000 high shear homogenizer (CAT Scientific Inc., USA) until a homogenous mineralized Nano-cellulose hydrogel was obtained. The mineralized hydrogel was then injected into cylindrical Teflon molds 2 mm depth and 5 mm diameter. The molds enclosing the mineralized hydrogel were stored in a freezer at a temperature of approximately -20 °C for at least 24 h prior to freeze-drying, which was conducted for another 24 hours using a freeze dryer (Telstar, Lyoquest - 55 Plus, Spain) at a temperature of -40 °C and a vacuum of 0.5 mBar.

Surgical procedure The 18 rabbits were anesthetized with an injection of ketamine hydrochloride 50 mg/kg (Umedica Laboratories Pvt., Ltd., India) combined with Xylazine Hydrochloride 3 mg/kg (Xylaject, Adwia Pharmaceuticals Co., Egypt). The surgical site (rabbit thighs) was prepared for surgical intervention by being shaved carefully then disinfected by povidone Iodine 10% antiseptic solution (Betadine, Mundipharma Egypt LLC) (*Nam et al, 2014*). A 4 cm incision was made in both legs to expose the tibia bones of all rabbits. A rounded surgical sterile #2 round bur (Dentsply/Maillfer cooperation, Zurich, Switzerland) at a low speed was used to create two circular full cortical bone defects in each tibia, 8 mm apart, with 5 mm diameter and 2 mm depth under copious saline irrigation, resulting in four bone defects in each animal. (*Delgado-Ruiz et al, 2014*)

Study groups Each rabbit contains the four main groups of the study; (Figure 1)

Group A (Control group) Defects were left to heal spontaneously after suturing, without filling them by a graft material. (Negative control)

Group B (Material group) Defects were filled with the mineralized Nano-cellulose bone graft material and stabilized by suture.

Group C (Combination group) Defects were subjected to diode laser 650 nm, then filled with the mineralized Nano-cellulose bone graft material, and stabilized by suture.

Group D (Laser group) Defects were subjected to diode laser 650 nm before suturing.

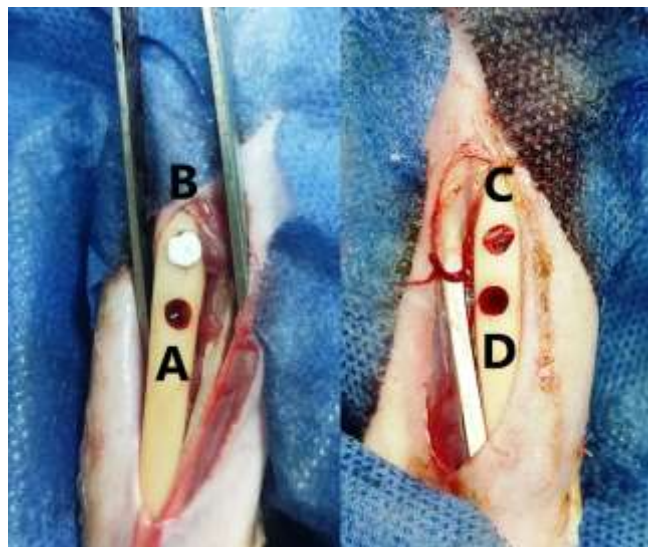


Figure (1) Photographs showing the four groups of the study
A (Control group), B (Material group), C (Combination group) and D (Laser group)

Laser Parameters & technique A diode laser device manufactured at the National Institute of Laser Enhanced Sciences (NILES), Cairo University (S.N.15012) 650 nm was used in a continuous and contact mode with 150 mw output power for 80 seconds (12 J/cm^2) with 6 mm diameter of the working probe of the hand piece. (*Abdallah Sabry et al, 2021*). In groups C and D, the first laser irradiation was applied to the defect after surgery, before graft material insertion and suturing. Then other laser irradiation sessions were applied superficially over the defect position every other day for two weeks, for a total of seven laser irradiations per defect. (*Barbosa et al, 2014*)

Post-Operative procedures Defects were sutured using sterile braided black polyester suture size 2/0 (Mersilene, Ethicon Ltd. UK), then topical antibiotic aerosol powder spray (Neomycin sulphate + Bacitracin zinc) was applied to the skin. (Bivatracin, Acdima trading, Giza, Egypt). To minimize the risk of infection after surgery, Amoxicillin + Flucloxacillin prophylactic antibiotic was injected for three days (Flumox 500 mg, Eipico, Egypt). Post-operative pain control was done using diclofenac sodium 75 mg injections for three days. (Cataflam, Novartis Pharma S.A.E., Cairo) The rabbits were sacrificed after two weeks and one month, by using a 100 mg/kg overdose of sodium pentobarbital 65 mg/ml (Altabarak 10st Alkopa, Cairo, Egypt). (*Nassar et al, 2022*)

Sample preparation & histological evaluation Tibial bones were removed, fixed in 10% buffered formalin, decalcified, cut by bone saw to identify the different groups, embedded in paraffin wax blocks, then 5 micron paraffin sections of each block were cut using a microtome for qualitative and quantitative histological evaluation. All groups were evaluated for new bone formation & defect healing, and examined by Masson Trichrome stain. Image analysis was conducted to obtain the area percent of new bone formation and amount of osteoid. (*Gurler & Gursoy, 2018*)

Capturing microscopic images were done using SOPTOP EX20 biological microscope (China), HD camera (model No. XCAM1080PHB) and Imageview software. Decalcified Masson Trichrome stained sections images were examined using the image analyzer computer system applying ImageJ software. Area percent of osteoid (blue color) formed in the defect area was measured in five fields per case using X100 magnification power. All fields were measured in a standard frame area of $2.0736 \times 10^6 \mu\text{m}^2$.

Statistical analysis

All results were collected, tabulated and statistically analyzed. Statistical analysis of the results was performed using SPSS software and represented in the form of mean \pm standard deviation values. Shapiro-Wilk test of normality was used to test normality hypothesis of the variables. Analysis of variance (ANOVA) test was used for evaluation of statistical significance of each parameter within the studied groups ($P < 0.05$), followed by Tukey Kramer Post hoc test for the statistically significant results. (*Mishra et al, 2019*)

Results

Histological Analysis

After two weeks: (Figure 2)

In the control group A, subjects showed partial closure of the defect with haphazardly arranged woven bone trabeculae. Masson Trichrome staining revealed many osteoid areas that stain blue, indicating they were freshly deposited without calcification.

In Material group B and combination group C, all subjects didn't show complete or even partial closure of the defect, instead they showed formation of woven bone trabeculae in the bottom and periphery of the defect. All subjects retained the graft material without resorption. Masson Trichrome staining revealed that all of the newly formed bone trabeculae were un-calcified osteoid in nature.

In laser group D, all subjects showed partial closure of the defect with woven bone trabeculae. Moreover, all subjects showed dilated blood vessels and mild inflammation. Bone trabeculae were lined with osteoblasts and showed many reversal lines indicating active remodeling into lamellar bone figure. MCT staining revealed that many areas of the newly formed bone trabeculae were un-calcified osteoid in nature.

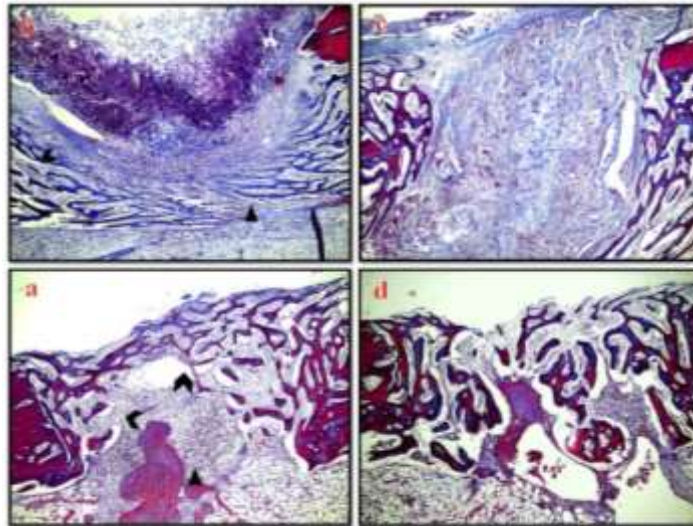


(Figure 2) Microscopic image of defects in the 4 groups after 2 weeks by Masson Trichrome stain, X40, showing:
(a) Partial closure of the defect with woven bone, with many areas of osteoid (blue colored trabeculae).
(b) Osteoid formation (blue colored trabeculae) at the base of the defect.
(c) Woven bone formation at the sides of the defect with many areas of osteoid (blue colored trabeculae), the center of the defect was filled with residual material.
(d) Partial closure of the defect with woven bone with areas of osteoid (blue colored trabeculae)

After one month: (Figure 3)

In the control group A, the subjects showed complete closure of the defect with lamellar bone that showed many reversal lines and remnants of woven bone. Masson Trichrome staining revealed few areas of osteoid that stain blue.

In group B and group C, all subjects showed partial closure starting from the top of the defect. The formed bone showed many reversal lines with remnants of woven bone figure. All subjects retained the graft material without resorption in the bottom of the defect for group B, and in the center of the defect for group C. Masson Trichrome staining revealed that most of the newly formed bone trabeculae were uncalcified osteoid in nature.

In laser group D, all subjects showed complete closure of the defect with lamellar bone trabeculae, which were lined with osteoblasts and showed many reversal lines and osteoclasts indicating active remodeling. Masson Trichrome staining revealed that few areas of the newly formed bone trabeculae were uncalcified osteoid in nature.

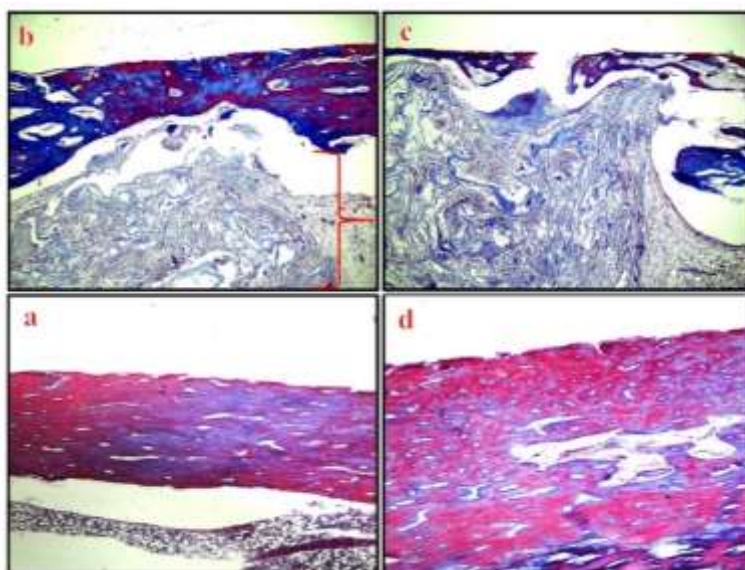


(Figure 3) Microscopic image of defects in the 4 groups after 1 month by Masson Trichrome stain, X40, showing:
(a) Complete closure of the defect with lamellar bone with little areas of osteoid (blue color)
(b) Partial closure of the defect with lamellar bone with many areas of osteoid (blue color), residual material was present in the base of the defect (bracket).
(c) Woven bone formation at the roof of the defect with areas of osteoid (blue color), residual material was present at the center of the defect.
(d) Complete closure of the defect with lamellar bone with little areas of osteoid (blue color).

Quality of newly formed bone: (Masson trichrome stain osteoid area percent)

Two weeks: Group D had the highest mean area percent of osteoid, whilst group C recorded the lowest value. The results of the one-way analysis of variance (ANOVA) test showed that there was no statistically significant difference between any of the groups. ($P > 0.05$) (Figure 4)

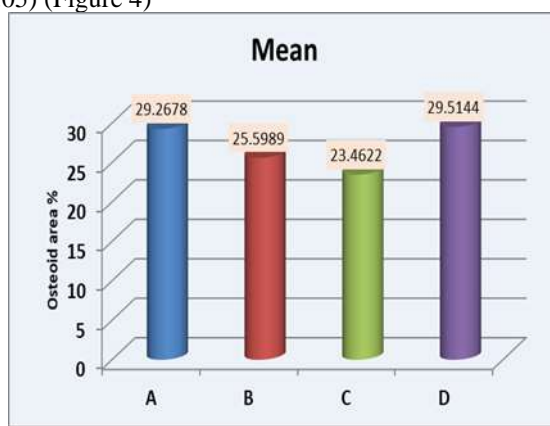


(Figure 4) Column chart showing two weeks area percent of osteoid formation in all groups.

One month: Group B showed the highest mean area percent of osteoid, whereas group C recorded the lowest number. The difference between all groups was statistically significant ($P < 0.05$) according to the one way analysis of variance (ANOVA) test. Tukey's post hoc analysis only found a significant difference between groups B and C. (Figure 5)

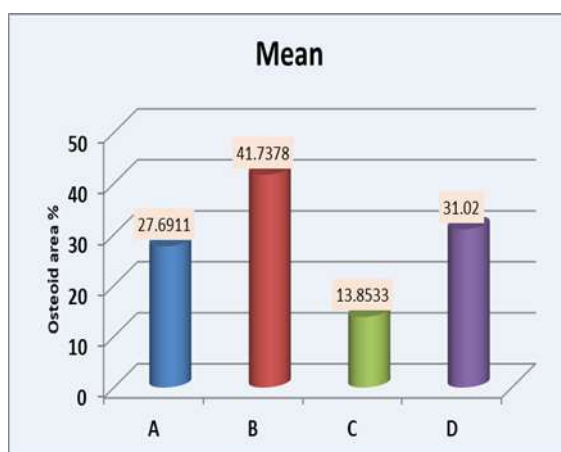


(Figure 5) Column chart showing one month area percent of osteoid formation in all groups.

Discussion

The current experimental study aimed to evaluate the effect of LLLT, mineralized Nano-cellulose graft material, and a combination of both, on bone healing in rabbit tibias. It also compared those three treatment modalities with a negative control group.

Bony defects of the jaws occur for various reasons, spontaneous bone regeneration in untreated defects is limited to a small distance depending on the size, because of the much more rapid proliferation of the surrounding soft tissues. Bone regeneration techniques can be incorporated into this process to assist or stimulate bone growth. (Arvidson et al, 2011; Qu et al, 2012)

The regeneration of defective bone always follows the same pattern, during the healing process, three phases can be distinguished that build on each other and occur in sequence: early healing, biological bone formation, and remodeling. The ideal graft material should resorb in time to permit and promote the growth of new bone, while maintaining its properties as an osteo-conductive scaffold until its purpose is fulfilled. (Acar et al, 2016)

Autogenous bone grafts were always considered as a golden standard for bone regeneration. However, their use is difficult and diminished because of many factors such as quantity obtained, their harvesting techniques, unpredictable resorption, and need for a second surgical site. Next in line were the allografts and xenografts, which have been widely used for different bone regeneration procedures. Yet again, their use was faced with many problems such as immunological reactivity and risk of disease transmission. Hence, synthetically derived bone graft materials were the next most practical step, known as alloplasts. (Jain et al, 2012)

The use of artificial bone graft substitutes has grown more popular, as the surgical application increases, and the availability of allograft bone decreases. They were found to be biocompatible, biodegradable, osteo-conductive, safe and non-toxic. They also exhibited angiogenesis, hemostasis and barrier membrane properties. (Ruga et al, 2011; Jain et al, 2012)

There has been Continuous attempts to create new bone graft materials with improved bioactivity for tissue engineering purposes, using composites of cellulose Nano-materials and calcium phosphate particles. (Qu et al, 2012; Acar et al, 2016)

Cellulose-based hydrogels combine the benefits of being biocompatible, non-toxic, and of low cost. (Chang and Zhang, 2011; Yao and Xu, 2014)

A positive alkaline phosphate assay revealed that the Nano-cellulose hydrogel made from rice straw was biocompatible in terms of its non-toxic impact on osteoblast-like cells, and its capacity to promote ossification. The produced Nano-fibers can be employed as an alternative to other cellulose derivatives due to their strong gel property, non-toxicity, and bioactivity. (Safwat et al, 2018)

Bioceramics were incorporated into polymeric materials to develop composite materials for bone regeneration. The proliferation, differentiation, and attachment of osteoblasts & mesenchymal stem cells (MSCs) were improved through such efforts. Biphasic calcium phosphate (BCP), the gold standard of bone substitutes made of a mixture of two distinct calcium phosphate phases—hydroxyapatite (HA) and Tricalcium phosphate (TCP)—at various ratios, is one of the bioactive ceramic materials. HA is a biocompatible, osteo-conductive, and osteophilic substance, making it useful in composites for replacing missing bone. TCP exhibits a high degree of chemical purity and homogeneity; as a result, its biological effects may be reliably predicted. (Leotot et al, 2015; Acar et al, 2016)

Tetramethyl pyridine oxyl (TEMPO) oxidized Nano-fibrillated cellulose extracted from rice straw, mixed with biphasic Tricalcium phosphate, proved to be a successful bone graft material. (*Safwat et al, 2018*)

In the current study, the hydrogel material was subjected to freeze-drying into discs form, for better handling, insertion and retention properties when used as a bone graft material. (*Zimmermann et al, 2016*)

LLLT (Low Level Laser Therapy) is the application of red and near infra-red light over injuries or lesions to ameliorate wound & soft tissue healing, reduce inflammation and give relief for both acute and chronic pain. Increased speed, quality, and tensile strength of tissue repair are achieved by the application of LLLT, consequently promoting the healing process. (*Blaya et al, 2008*)

Laser biomodulating activity was initially referred to as biostimulation. Biomodulation may be accomplished utilizing more compact, practical lasers used at low power settings (1 to 500 mW). These devices have been reported in the literature under a variety of names, including low-level laser, soft laser, and therapeutic laser. (*De Souza et al, 2012*)

Low-level laser therapy (LLLT) has grown significantly in popularity and significance as a treatment option for a variety of illnesses, including bone restoration procedures, musculoskeletal complications, and pain management. (*Torres et al, 2008; Klemm et al, 2011*)

Rabbit ranks top among all the animals used for musculoskeletal research and is one of the most often utilized animal models. Rabbits are easily available, easy to house and handle, and they have faster skeletal change and bone turnover. Reports showed that there were resemblance in bone mineral density and the fracture toughness of mid-diaphyseal bone between rabbits and human. This makes rabbits the first choice for animal model research for the in-vivo test of a new bone substitute biomaterials. (*Ye Li et al, 2015*)

Histological evaluation is the most powerful method to evaluate the healing of bone defects, and considered a direct method for testing the biocompatibility. (*Mohammed et al, 2019*)

In bone histology Masson's trichrome staining is a widely used method, it enables both morphological and color-based tissue identification. (*Rentsch et al, 2014*)

After two weeks evaluation period, group D (Laser group) recorded the greatest mean area percent of osteoid, followed by group A (control group). All subjects in both groups showed partial closure of the defect with woven bone trabeculae, and Masson's Trichrome staining revealed that many areas of the newly formed bone trabeculae (blue stained) were uncalcified osteoid in nature.

For (group D), the recorded increase in osteoid formation can be explained according to *Neto et al, 2021* due to the effect of laser photobiostimulation on bone healing process, which increases the synthesis of ATP synthetase, hence promoting nucleic acid production, and accelerates cell division. By having a positive impact on the bone matrix and producing highly reactive and vital bone tissue, low-power laser irradiation considerably increases the number of viable osteocytes in the irradiated bone in hard tissues. While *Atasoy et al, 2017* disagreed with the above findings, suggesting that LLLT might not speed-up the bone repair process in both the initial and the late phases of healing.

The high osteoid formation in (group A) meet the findings by (*Faot et al, 2017 and Ou et al, 2020*) stating that there was an increase in bone healing in rabbits without incorporating a bone graft material, this could be explained by the three phases of bone healing process; early healing, biological bone formation, and remodeling.

While groups B (material group) and C (combination group) showed considerably lower values of mean area percent of osteoid, compared to the other test groups. All subjects in both groups showed partial closure starting from the top of the defect, and retained graft material without resorption in the center and bottom of the defect. Masson Trichrome staining revealed that most of the newly formed bone trabeculae were uncalcified osteoid in nature. that could be due to the mineralized component of the material (biphasic Tricalcium phosphate), that was found to have slow or delayed effect on bone healing during the first two weeks of application, as mentioned in a study by *Shamma et al, 2017*.

After one month evaluation period, laser group D and control group A showed complete closure of the defects by woven bone lined with osteoblasts, and showed many reversal lines and osteoclasts indicating active remodeling into lamellar bone. Masson Trichrome staining revealed few areas of the newly formed bone trabeculae were uncalcified (blue stained) osteoid in nature. The mean area percent of osteoid in group D was higher than in group A, suggesting that LLLT accelerates the bone healing process, in comparison to the control group A. These results are in agreement with the finding of (*Aoki et al, 2004*) who reported that, a diode laser with a wavelength of 655nm to 980 nm can accelerate wound healing, promote angiogenesis, increase growth factor release, and decrease inflammation. (*Khalil & Mahmoud, 2010*)'s findings showed complete bone defects repair at day 28 postoperatively, suggesting that laser stimulates cell proliferation by increasing growth factors' production, oxygen uptake by the cell, and ATP synthesis in mitochondria. This was also in accordance with the outcome of studies conducted by (*Seifi et al, 2012; Allahverdi et al, 2014; El-Hayes et al, 2016; Nazht et al, 2018; Neto et al, 2021*).

Groups B and C showed partial closure of the defects. All subjects retained the graft material without resorption, in the bottom of the defect for group B, and in the center of the defect for group C. Masson Trichrome staining revealed that

most of the newly formed bone trabeculae were uncalcified osteoid in nature. The highest mean area percent of osteoid was recorded in material group B, whereas combination group C recorded the lowest value.

The graft material retention and delayed healing in group C can be attributed to HA's low osteo-conductive activity and a good space-maintaining ability, whereas Beta-TCP is more bio-resorbable and is rapidly replaced by new bone. This relation makes part of the graft being resorbed rapidly (TCP) while the (HA) remains in situ for a longer period, in accordance with a study by *Soares et al, 2014*. Another explanation for graft material retention, is that it might have acted as a physical barrier for the penetration of the laser radiation, leading to the decrease of laser effect on the healing process, as suggested by *Bigueti et al, 2012*. Moreover, laser 650 nm might have affected the resorption process of the graft material in group C, such assumption was developed when observing group B results, which had higher resorption pattern of the material, with a noticeable increase in new bone formation, in the form of osteoid, in accordance with the study by *Toloue et al, 2012*, stating that the osteo-conduction of bone substitute requires the material to possess a resorption rate identical to that of new bone formation

On the other hand, Group B showed delayed new bone formation with the highest mean area percent of osteoid when compared to other groups in both evaluation periods, suggesting that the experimental material's bone repair capacity increased throughout the study intervals, that could be explained by the unique combination used in the current bone graft material as found by *Safwat et al, 2020*, highlighting the favorable effect of using CNF hydrogel together with nACP on bone formation, where Nano-cellulose hydrogel prepared from rice straw proved to have the power to evoke ossification as indicated by the positive alkaline phosphate assay. The presence of CNF (cellulose Nano fibrils) with its bioactive role and the known ability of the hydrogel to confine and maintain a high concentration of the loaded active ingredient at the implantation site over an extended period of time, might play a role in increasing the level of bone formation.

Conclusion

Diode laser 650 nm biostimulation improved the healing and repair of bone defects. TEMPO-oxidized Nano-cellulose combined with Nano amorphous calcium phosphate showed a delayed effect in bone healing and graft material resorption. The combination of LLLT with the experimental mineralized Nano-cellulose material had no positive effect on bone defect healing.

Recommendations

Further investigations are needed to improve the biological effect and physical properties of the experimental material along with incorporating different wavelengths of diode laser. Other methods of assessment are advised to verify the findings of the present study.

References

1. *Abdallah Sabry M, Saafan AM, El-Shennawy HM, Hussine AA, El-Aziz A, Mohamed D, Abdel Fadeel DA*. The Efficiency of Photodynamic Therapy in the Management of Pain in Patients with Oral Lichen Planus. *Journal of Chemical Health Risks*. 2021 Oct 1;11(Special Issue: Bioactive Compounds: Their Role in the Prevention and Treatment of Diseases):189-96.
2. *Acar AH, Yolcu Ü, Altındiş S, Gül M, Alan H, Malkoç S*. Bone regeneration by low-level laser therapy and low-intensity pulsed ultrasound therapy in the rabbit calvarium. *Archives of Oral Biology*. 2016 Jan 1;61:60-5.
3. *Allahverdi A, Sharifi D, Abedi G, Hesarakı S, Fattahiyani H*. Effect of platelet-rich plasma, low-level laser therapy(650 nm) or their combination on the healing of Achilles tendon in rabbits: a histopathological study. *Eur. J. Exp. Biol*. 2014;4(3):201-8.
4. *Aoki A, Sasaki KM, Watanabe H, Ishikawa I*. Lasers in nonsurgical periodontal therapy. *Periodontology 2000*. 2004 Oct 1;36(1):59-97.
5. *Arvidson K, Abdallah BM, Applegate LA, Baldini N, Cenni E, Gomez-Barrena E, Granchi D, Kassem M, Kontinen YT, Mustafa K, Pioletti DP*. Bone regeneration and stem cells. *Journal of cellular and molecular medicine*. 2011 Apr;15(4):718-46.
6. *Atasoy KT, Korkmaz YT, Odaci E, Hanci H*. The efficacy of low-level 940 nm laser therapy with different energy intensities on bone healing. *Brazilian oral research*. 2017 Jan 5;31.
7. *Bigueti CC, Filho EJ, de Andrade Holgado L, Caviquioli G, Moreschi E, Comparin E, Matsumoto MA*. Effect of low-level laser therapy on intramembranous and endochondral autogenous bone grafts healing. *Microscopy research and technique*. 2012 Sep;75(9):1237-44.
8. *Barbosa D, Villaverde AGJB, Loschiavo Arisawa EA, Souza RA de*. Laser therapy in bone repair in rats: analysis of bone optical density. *Acta ortopedica brasileira*. 2014;22:71-4.
9. *Blaya D, Guimarães M, Pozza D, Weber J, Oliveira M*. Histologic Study of the Effect of Laser Therapy on Bone Repair. *The Journal of Contemporary Dental Practice*. 2008; (9)6:41-48.
10. *Chang C and Zhang L*.: Cellulose-based hydrogels: present status and application prospects. *Carbohydr Polym*. 2011;(84): 40-53.
11. *Delgado-Ruiz RA, Calvo-Guirado JL, Abboud M, Ramirez-Fernández MP, Maté-Sánchez JE, Negri B, Won A, Romanos G*. Porous titanium granules in critical size defects of rabbit tibia with or without membranes. *International Journal of Oral Science*. 2014 Jun;6(2):105-10.
12. *De Souza M, Medeiros V, Toma L, Reginato R, Katchburian E, Nader H, Faloppa F*. The low level laser therapy effect on the remodeling of bone extracellular matrix. *Photochemistry and Photobiology*. 2012 Sep;88(5):1293-301.
13. *El-Hayes KA, Zaky AA, Ibrahim ZA, Allam GF, Allam MF*. Usage of low level laser biostimulation and platelet rich fibrin in bone healing: Experimental study. *Dental and Medical Problems*. 2016;53(3):338-44.
14. *Faot F, Deprez S, Vandamme K, Camargos GV, Pinto N, Wouters J, van den Oord J, Quirynen M, Duyck J*. The effect of L-PRF membranes on bone healing in rabbit tibiae bone defects: micro-CT and biomarker results. *Scientific reports*. 2017 Apr 12;7(1):1-0.
15. *Gurler G, Gursoy B*. Investigation of effects of low level laser therapy in distraction osteogenesis. *Journal of stomatology, oral and maxillofacial surgery*. 2018 Dec 1;119(6):469-76.

16. **Hou X, Zhang L, Zhou Z, Luo X, Wang T, Zhao X, Lu B, Chen F, Zheng L.** Calcium Phosphate-Based Biomaterials for Bone Repair. *Journal of Functional Biomaterials*. 2022 Oct 14;13(4):187.
17. **Jain A, Chaturvedi R, Pahuja B.** Comparative evaluation of the efficacy of calcium sulfate bone grafts in crystalline and nano-crystalline forms in fresh extraction socket sites: A radiographic and histological pilot study. *Int. J. Oral Implantol. Clin. Res.* 2012;3:58-61.
18. **Khalil RA, Mahmood AS.** Evaluation the Effect of 805 nm Wavelength Diode Laser on Repair of Mandibular Bone Repair and Skin Incisions in Rabbits. *Iraqi Journal of Laser*. 2010 Dec 15;9(B):17-22.
19. **Klemm D, Kramer F, Moritz S, Lindström T, Ankerfors M, Gray D, Dorris A.** Nanocelluloses: a new family of nature-based materials. *Angewandte Chemie International Edition*. 2011 Jun 6;50(24):5438-66.
20. **Léotot J, Lebouvier A, Hernigou P, Bierling P, Rouard H, Chevallier N.** Bone-forming capacity and biodistribution of bone marrow-derived stromal cells directly loaded into scaffolds: a novel and easy approach for clinical application of bone regeneration. *Cell Transplantation*. 2015 Oct;24(10):1945-55.
21. **Mishra P, Pandey CM, Singh U, Gupta A, Sahu C, Keshri A.** Descriptive statistics and normality tests for statistical data. *Annals of cardiac anaesthesia*. 2019 Jan;22(1):67.
22. **Mohammed AA, Saleh RG, Taiema DA, Abdel-Hady AN, Metwally A.** In Vivo Biocompatibility of β Tri-calcium Phosphate Versus White Portland Cement in Mandibular Bone Surgical Defect in Dogs. *Egyptian Dental Journal*. 2019 Oct 1;65:3475-3485.
23. **Nam NH, Sukon P, Tangkawattana S, Suthiprapaporn P, Rattana-archa P, Kampa N.** Stimulatory Effects of Low Intensity Laser Therapy on the Healing of Rabbit Tibial Defects. *The Thai Journal of Veterinary Medicine*. 2014 Dec 1;44(4):487.
24. **Nassar M.A, Abdelgawad L.M., Khallaf M.E., El Rouby D.H., Sabry D., Radwan M.M.** Efficacy Of Photobiomodulation Using 870 Nm Diode Laser, Experimental Nano Calcium Aluminate/Tri Calcium Silicate Material And MTA In Furcal Perforation Repair. (Animal Study) *Neuro Quantology*. 2022; 20(14):1056-1064.
25. **Nazht HH, Omar RA, Aldahhan MR.** Effect of Low Level Laser Therapy on the Sheep Ribs Xeno Graft in the Treatment of Rabbits Long Bone Fractures. *Arts, Humanities and Natural Sciences Conferences*, Aug 25, 2018.
26. **Neto dos Santos OM, Lilge L, Damante CA, Campos AC, Issa JP.** Effects of Photobiomodulation on Experimental Bone Repair in Animal models: a Systematic Review. *Journal of Morphological Sciences* Vol. 2021;38:224..
27. **Ou KL, Hou PJ, Huang BH, Chou HH, Yang TS, Huang CF, Ueno T.** Bone healing and regeneration potential in rabbit cortical defects using an innovative bioceramic bone graft substitute. *Applied Sciences*. 2020 Sep 8;10(18):6239.
28. **Qu P, Wang X, Cui XX.** Biomimetic mineralization of rod-like cellulose nano-whiskers and spectrum analysis. *Spectrosc Spectral Anal*. 2012 May 1;32(5):1418-22.
29. **Rentsch C, Schneiders W, Manthey S, Rentsch B, Rammelt S.** Comprehensive histological evaluation of bone implants. *Biomater*. 2014 Jan 17;4(1):e27993.
30. **Ruga E, Gallezio C, Chiusa L, Boffano P.** Clinical and histologic outcomes of calcium sulfate in the treatment of postextraction sockets. *Journal of Craniofacial Surgery*. 2011 Mar 1;22(2):494-8.
31. **Safwat E, Hassan ML, Saniour S, Zaki DY, Eldeftar M, Saba D, Zazou M.** Injectable TEMPO-oxidized nanofibrillated cellulose/biphasic calcium phosphate hydrogel for bone regeneration. *Journal of biomaterials applications*. 2018 May;32(10):1371-81.
32. **Safwat EM, Sharaf NF, Farrag ARH, Hassan ML, Zaki DY.** Osseous Regeneration of Periapical Lesions using Rice Straw Nanofibers-Nano Amorphous Calcium Phosphate Composite Hydrogel (In Vivo Study). *J Mol Nanot Nanom*. 2020 2(1): 109.
33. **Shamma MM, Ayad SS, El-dibany RM, Nagui DA.** Evaluation of the effect of hyaluronic acid mixed with biphasic calcium phosphate on bone healing around dental implants (experimental study). *Alexandria Dental Journal*. 2017 Apr 1;42(1):104-7.
34. **Seifi M, Atri F, Yazdani MM.** Effects of low-level laser therapy on orthodontic tooth movement and root resorption after artificial socket preservation. *Dental research journal*. 2014 Jan;11(1):61.
35. **Soares LG, Marques AM, Guarda MG, Aciole JM, dos Santos JN, Pinheiro AL.** Influence of the λ 780 nm laser light on the repair of surgical bone defects grafted or not with biphasic synthetic micro-granular hydroxylapatite+ beta-calcium triphosphate. *Journal of Photochemistry and Photobiology B: Biology*. 2014 Feb 5;131:16-23.
36. **Toloue, S.M.; Chesnoiu-Matei, I.; Blanchard, S.B.** A Clinical and Histomorphometric Study of Calcium Sulfate Compared with Freeze-Dried Bone Allograft for Alveolar Ridge Preservation. *J. Periodontol*. 2012 83;847-855.
37. **Torres CS, dos Santos JN, Monteiro JS, Amorim PG, Pinheiro AL.** Does the use of laser photobiomodulation, bone morphogenetic proteins, and guided bone regeneration improve the outcome of autologous bone grafts? An in vivo study in a rodent model. *Photomedicine and Laser surgery*. 2008 Aug 1;26(4):371-7.
38. **Yao WR, Xu QH.** Research progress in nanocellulose preparation. *Advanced Materials Research*. 2014;988:101-5.
39. **Ye Li, Chen SK A, Long Li A, Ling Qin AC, Xin-Luan Wang AC, Lai XY.** Bone defect animal models for testing efficacy of bone substitute biomaterials. *Journal of orthopaedic translation*. 2015 Jul 1;3(3):95-104.
40. **Zimmermann MV, Borsoi C, Lavoratti A, Zanini M, Zattera AJ, Santana RM.** Drying techniques applied to cellulose nanofibers. *Journal of Reinforced Plastics and Composites*. 2016 Apr;35(8):628-43